Using the E-CDF-S and COMBO-17 to Examine the X-ray-to-Optical Properties of Optically-Selected Active Galaxies

A.T. Steffen (PSU), I. Strateva (PSU), W. N. Brandt (PSU), D. M. Alexander (IoA), A. Koekemoer (STScI), B. Lehmer (PSU), D. P. Schneider (PSU), C. Vignali (INAF)

Abstract

Using the optically-selected AGN from the COMBO-17 survey of the E-CDF-S field (which extends 3 magnitudes fainter than the SDSS) and the corresponding E-CDF-S X-ray data, we supplement more luminous optically-selected AGN surveys and compile a relatively homogeneous sample of 332 optically-selected, radio-quiet, unabsorbed AGN with the largest X-ray detection fraction to date (88%). Using partial correlation analyses we confirm that the UV emission of AGN is strongly correlated with their soft X-ray emission (15.3σ) while controlling for the effects of redshift. The UV-to-X-ray emission ratio, $\alpha_{ox}=0.384\log[l_{2\,keV}/l_{2500\,Å}]$, is related to the AGN luminosity (in the sense that less luminous AGN emit more soft X-rays per unit UV), but remains unchanged with cosmic time (<30% between z=0–5). Precise knowledge of this relationship is important for testing energy generation models of AGN, deriving bolometric corrections, identifying X-ray weak AGN, and comparing AGN luminosity functions derived from X-ray and optically-selected samples.

Samples

We assembled a sample of 332 optically-selected, radio-quiet AGN with correspondingly deep soft X-ray coverage (see Table 1). Our sample was chosen to cover a large area of the luminosity-redshift plane to minimize degeneracies (see Figure 1, below). Optical spectra were used, when available, to identify and remove AGN with broad UV absorption lines (BALs). By removing the radio-loud and BAL AGN we ensure that our observations measure the intrinsic rest-frame UV and soft X-ray emission of AGN. To our knowledge, this is the cleanest (controlling for RL, BAL, host-galaxy contribution, etc.) sample of optically-selected AGN with the highest X-ray detection fraction (88%) to date.

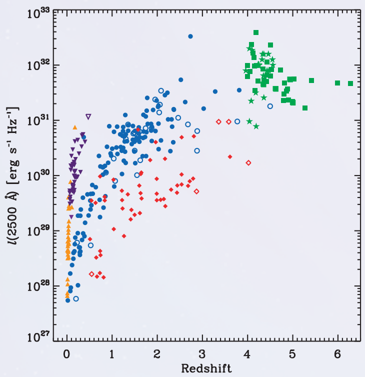

Figure 1. Distribution of UV monochromatic luminosities with redshift. The inclusion of both large area and deep, pencil-beam samples allows us to break the strong luminosity–redshift correlation characteristic of flux-limited samples without compromising the X-ray detection fraction. X-ray upper limits are indicated with open symbols (in this plot only). Symbols are defined in Figure 2.

Statistical Tools

While our sample provides good coverage of the luminosity-redshift plane, both the UV and X-ray luminosities are still correlated with redshift. To measure the strength of correlations between $l_{2500\,Å}$, $l_{2\,keV}$, α_{OX}, and redshift, we use partial correlation methods, which measure the correlation between any two variables while controlling for the effects of a third. We use rank correlation coefficient analysis, developed by Akritas and Siebert (1996), which accounts for the presence of censored data.

To obtain the linear regression parameters, we use the Astronomy Survival Analysis package (ASURV, La Valley et al. 1992, Isobe et al. 1985).

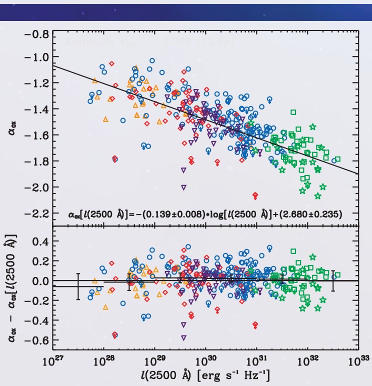

Figure 3. The X-ray-to-UV index, α_{OX}, is anti-correlated with the UV monochromatic luminosity. X-ray upper limits are indicated with arrows. Luminous AGN emit fewer X-rays per unit UV luminosity than less luminous AGN. Symbols are

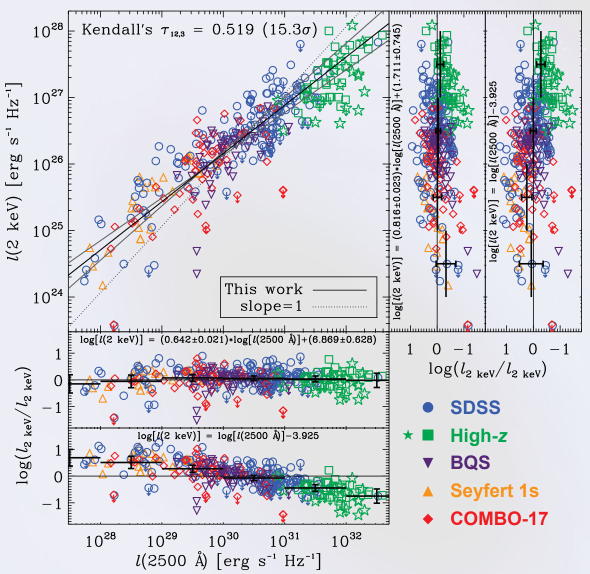

Figure 2. Rest-frame 2 keV monochromatic luminosity versus rest-frame 2500 Å monochromatic luminosity. The symmetric, best-fit relationship is denoted by a solid, black line. The solid, gray lines are the best-fit lines reducing the residuals for only one variable. The residuals for the fit reducing only the $l_{2\,keV}$ ($l_{2500\,Å}$) residuals are given in the bottom (right) plots, along with the residuals using a β=1 slope. The symbols are defined in the lower-right corner.

Table 1. Samples

Number of AGN	% X-ray Detected	Area [deg^2]	Optical/UV Survey	X-ray Survey	X-ray Exposure [ks]	X-ray Limit [erg s^{-1} cm^{-2}]
155	81	15	SDSS	ROSAT PSPC	12–66	10^{-14}
52	**90**	**0.26**	**COMBO-17**	**E-CDF-S**	**≈ 250**	$\mathbf{10^{-16}}$
46	98	10,714	BQS	ROSAT	0.5-25	10^{-12}
54	94	...	SDSS/PSS/APM	Chandra/XMM	5–40	10^{-15}
30	100	...	IUE	RASS	≈ 0.5	10^{-12}

SDSS -- Sloan Digital Sky Survey (Data Release 2; York et al. 2000)
BQS -- Bright Quasar Survey (Schmidt & Green 1983)
PSS -- Palomar Digital Sky Survey (Djorgovski et al. 1998)
APM -- Automatic Plate Measuring (Irwin et al. 1991)
IUE -- International Ultravoilet Explorer
ROSAT -- RÖntgen SATellite
PSPC -- Position Sensitive Proportional Counter
E-CDF-S -- Extended Chandra Deep Field South (Lehmer et al. 2005)
XMM -- X-ray Multiple mirror Mission - Newton
RASS -- ROSAT All Sky Survey

Results from Steffen et al. (2006; submitted to AJ) and Strateva et al. (2005).

We gratefully acknowledge support from NSF CAREER award AST-9983783 (A.T.S. and W.N.B.), NASA LTSA grant NAG5-13035 (I.S. and W.N.B.), CXC grant G04-5157A (A.T.S., W.N.B., B.D.L., and D.P.S), the Royal Society (D.M.A), and MIUR COFIN grant 03-02-23 (C.V.)

No Redshift Evolution

Using the α_{ox} residuals as a function of redshift (see the top panel of Figure 4, below) we estimate that the mean ratio of rest frame UV to soft X-ray emission has changed by less than 30% (1σ) over the redshift range probed (0.01<z<5).

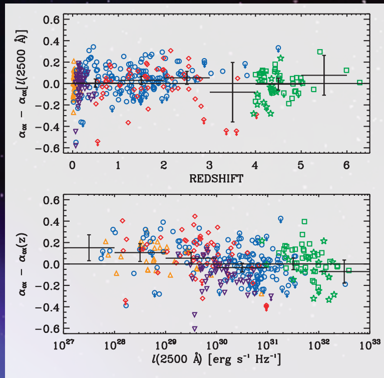

Figure 4. α_{OX} residuals, assuming luminosity (top) or redshift (bottom) dependence only. The overlaid error bars denote the mean and the 3σ standard deviation of the mean of the residuals calculated for each Δz =1 bin (top) or Δlog($l_{2500\,Å}$) = 1 bin (bottom). X-ray upper limits are indicated with arrows. Symbols are defined in Figure 2. Redshift dependence alone cannot explain the observed variation in α_{OX}, while luminosity dependence alone can.

Comparison with Earlier Studies

The α_{OX} - $l_{2500\,Å}$ correlation was first suggested in AGN studies performed in the early 1980s. While these studies found no correlation between α_{OX} and redshift, the heterogeneous AGN samples with low X-ray detection fractions (10-50%) yielded large errors. As seen in Figure 5 below, our study tightly constrains the α_{OX} parameters, conclusively showing no significant redshift dependence. To facilitate comparison we cast the $\alpha_{OX}(l_{2500\,Å},z)$ relation in terms used by Avni & Tananbaum (1996), where $\tau(z)$ is the fractional cosmological look-back time extending from today (τ=0) to the Big Bang (τ=1).

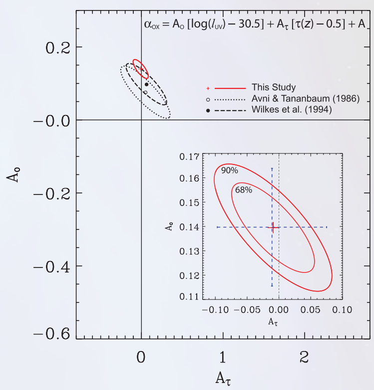

Figure 5. The confidence contours for our sample, and the samples examined by Avni & Tananbaum (1986) and Wilkes et al. (1994). The contours represent 90% confidence intervals considering two parameters of interest. Inset: A close-up of the 68% and 90% contours for our sample, compared to the best-fit and 2σ error range from ASURV (blue dotted line).

Results

- The rest-frame UV and X-ray luminosities of AGN are strongly correlated (15.3σ; Figure 2), controlling for the effects of redshift.
- We find the slope of the $l_{2500\,Å}$–$l_{2\,keV}$ correlation is less than one (β=0.73 ± 0.01; Figure 2).
- The primary dependence of α_{OX} is on $l_{2500\,Å}$ (13.5σ; Figure 3) and not z (1.2σ).
- The residuals of the best-fit α_{OX} - log($l_{2500Å}$) relation suggest this relation may be non-linear (Figure 3).
- We find a weaker, but significant correlation between α_{OX} and $l_{2\,keV}$ (3.0σ), controlling for the effects of redshift.
- The ratio of UV to X-ray emission of AGN has changed by less than 30% since the Universe was ~1 Gyr old (Figure 4).
- Less luminous AGN emit relatively more X-rays than their more luminous counterparts.
- Optical AGN surveys must cover a larger range in luminosity to observe the AGN population revealed in X-ray surveys.
- Our results imply that optical luminosity functions will undergo luminosity-dependant density evolution (LDDE) at faint optical magnitudes.